

UNDERGRADUATE
HONORS THESIS

Behavior of Minimum Length
Splices of High-Strength
Reinforcement

by

Kristen Donnelly

A thesis submitted in partial
fulfillment of the requirements for
the Undergraduate Honors Thesis
(ARE 679)

The University of Texas at Austin

2006-2007

ACKNOWLEDGMENTS

For their interest, encouragement and great patience with this project, I am very grateful for the contributions of Dr. James Jirsa, Greg Glass, and Brian Graves. Without their hard work, this study would not have been possible.

TABLE OF CONTENTS

1.0 INTRODUCTION.....	1
1.1 STATEMENT OF PURPOSE	1
2.0 LITERATURE REVIEW	3
2.1 MATERIAL PROPERTIES OF MMFX STEEL.....	3
2.2 DESIGN CONSIDERATIONS ESTABLISHED BY ACI	4
2.3 DESIGN CONSIDERATIONS FOR MMFX STEEL	4
2.4 COORDINATED STUDY OF MMFX BAR SPLICES	5
3.0 EXPERIMENTAL WORK	8
3.1 DESCRIPTION OF TEST SETUP AND SPECIMENS AS DESIGNED	8
3.2 CONSTRUCTION.....	11
3.3 TESTING.....	14
4.0 TEST RESULTS AND INTERPRETATION	15
4.1 RESULTS OF #5 MMFX TESTS COMPLETED IN THIS STUDY	15
4.1 RESULTS OF #5 MMFX TESTS (GLASS, 2007).....	18
4.3 INTERPRETATION OF RESULTS.....	18
5.0 APPLICATION TO PRACTICE	26
5.1 DESIGN RECOMMENDATIONS	26
6.0 SUMMARY AND CONCLUSIONS.....	27
BIBLIOGRAPHY	
APPENDIX A: EQUATIONS ESTABLISHED BY ACI 408R-03	
A.1 CHAPTER 1 -- BOND BEHAVIOR	
A.2 CHAPTER 4 -- DESIGN PROVISIONS	
APPENDIX B: EQUATIONS ESTABLISHED BY ACI 318-05	
B.1 CHAPTER 2 -- NOTATION AND DEFINITIONS	
B.2 CHAPTER 12 -- DEVELOPMENT AND SPLICES OF REINFORCEMENT	

LIST OF FIGURES

FIGURE 1: STRESS-STRAIN BEHAVIOR OF #5 AND #8 MMFX BARS (GLASS, 2006)	5
FIGURE 2: TEST SETUP	8
FIGURE 3: PLAN VIEW OF BEAM, CLOSE-UP OF SPLICE LENGTH, AND SECTION VIEW FOR BEAM C0	9
FIGURE 4: ELEVATION VIEW OF BEAM AND CLOSE-UP OF SHEAR SPAN	10
FIGURE 5: FORMWORK	12
FIGURE 6: REBAR CAGES	12
FIGURE 7: CLOSE-UP OF SPLICE REGION OF REBAR CAGES	13
FIGURE 8: CLOSE-UP OF STRAIN GAUGES	13
FIGURE 9: PLACEMENT OF CONCRETE AND FRESHLY FINISHED BEAMS	13
FIGURE 10: TEST SETUP	14
FIGURE 11: CLOSE-UP OF CONCRETE BEARING AREA	15
FIGURE 12: CLOSE-UP OF CRACKING WITHIN SPLICE REGION OF C0	16
FIGURE 13: CLOSE-UP OF CRACKING WITHIN SPLICE REGION OF C1	17
FIGURE 14: CLOSE-UP OF CRACKING WITHIN SPLICE REGION OF C2	17
FIGURE 15: LOAD-DEFLECTION CURVES FOR BEAMS C0, C1, AND C2	21

LIST OF TABLES

TABLE 1: DETAILS OF TEST SPECIMENS	11
TABLE 2: RESULTS OF #5 MMFX BEAM TESTS	15
TABLE 3: RESULTS OF #5 MMFX BEAM TESTS (GLASS, 2007)	18
TABLE 4: CONFINEMENT TERMS FOR PREDICTING FAILURE STRESSES	21

1.0 Introduction

1.1 Statement of Purpose

MMFX is a new type of steel being used in reinforced concrete applications. Providing much greater strength than conventional Grade 60 steel, MMFX is uncoated steel that varies from conventional steel in its microstructure. Attractive benefits of MMFX include corrosion resistance and ability to retain ductility with increased strength. Designers have yet to take full advantage of the material's greater stress capacity in general structural applications. The American Concrete Institute (ACI) building code limits maximum design stress to 80 ksi, approximately half of the strength of MMFX reinforcement. From a designer's standpoint, less steel could be used if the ACI stress limitation could be increased. Even though the unit cost of MMFX steel is higher than conventional steel, the cost could be offset by the reduction in area needed.

To realize the benefits of high-strength steel, data is needed to extend knowledge of the behavior of such steel beyond the range of Grade 60 to 80 that are currently used. In this study, the behavior of MMFX in splices within reinforced concrete beams was examined. Splices are needed when two reinforcing bars overlap each other to provide continuity of reinforcement. Force carried by the bars increases as splice length increases, until the yield stress of the steel is reached. At that point, no additional increase in bar force can be realized. The design philosophy is that bars should yield before the splice region fails. The intent was to determine if high-strength MMFX bars could be designed as conventional Grade 60 steel bars are designed.

The study reported here supplemented a large study of splices sponsored by MMFX Corporation and conducted at the University of Texas at Austin (UT), North Carolina State University (NCSU), and Kansas University (KU). At UT, 29 beams were tested and are being reported by Glass and Hoyt (Glass, 2006). The variables include bar size, concrete compressive strength, cover and spacing,

confinement (transverse reinforcement), and splice lengths. While Glass and Hoyt tested beams with various splice lengths, the minimum splice length permitted by ACI (12 in.) was not examined. In this study, several additional beams were tested to examine the capacity of splices with minimum lengths. Observing the behavior of MMFX bars in short splice regions provided interesting data regarding the appropriateness of designing high-strength steel reinforced members with a code intended for use in lower-strength applications. Design recommendations were then made based on the resulting information.

2.0 Literature Review

2.1 Material Properties of MMFX steel

Micro-Composite Multi-Structural Formable (MMFX) steel was developed to provide more resistance to corrosion than conventional Grade 60 Steel. Problems arise within conventional steel at a microstructural level due to material composition. Typical carbon steels are composed of carbides and ferrites, which are “chemically dissimilar materials” that destroy the steel from the inside out. The formations of these “microgalvanic cells,” which drive the corrosive reaction, are exacerbated in moist environments (MMFX, 2005). Minimizing microgalvanic cell formation, MMFX is composed of austenite and martensite, and is thus practically free of carbides (Dawood). The result is steel that is reported to be five times as corrosion resistant than Grade 60 steel (MMFX, 2005).

In addition to increased resistance to deterioration, the unique material composition of MMFX results in steel that is approximately two to three times as strong in tension as conventional Grade 60 steel that exhibits a yield stress at about 60 ksi (MMFX, 2005; Dawood). While carbon steels can be designed to have higher strength than Grade 60 steel, this increased strength is realized at the cost of ductility. MMFX achieves its greater strength and retains toughness, resulting in steel that exhibits ductile behavior (MMFX, 2005). However, MMFX does not exhibit a well-defined yield stress. As stress increases within MMFX steel bars, the stiffness of the bars remains fairly constant and then gradually lessens and the stress remains at a nearly constant level until failure occurs. Lack of a well-defined yield stress creates difficulty when designing with MMFX, as will be discussed later (Section 2.2). Because high strains are reached, larger crack widths will be developed. Questions regarding serviceability will need to be considered.

2.2 Design Considerations Established by ACI

As established in Section 9.4 (Design Strength for Reinforcement) of ACI 318-05, the design values for the yield stress of longitudinal and transverse reinforcing steel are limited to 80 ksi (ACI Committee 318, 2004). Consequently, the maximum value of stress allowed for designing members reinforced with MMFX will be significantly less than the actual maximum values of stress demonstrated in tensile strength tests. More recent design recommendations, regarding splice lengths and stress levels within the splice region of bars at failure, have been published by ACI Committee 408 (2003).

Regarding the determination of splice lengths in reinforced concrete members, empirical expressions have been developed from test results, as an accurate mechanics-based procedure has not yet been derived for development and splice strength (ACI Committee 408, 2003). All relevant equations can be found in Appendix A of this thesis. The failure stresses of spliced bars predicted by ACI 318-05 and ACI 408 were then compared to the actual failure stresses experienced during experimental testing to determine the accuracy of these predicted values.

2.3 Design Considerations for MMFX Steel

When designing concrete members reinforced with MMFX steel, the equations established by the American Concrete Institute (ACI) are intended to apply to steel with yield strength up to 80 ksi. Because MMFX can withstand stresses of approximately 160 ksi (Figure 1), the limit imposed by ACI is conservative with respect to strength. On the other hand, since MMFX does not exhibit a well-defined yield plateau, it is less ductile than conventional Grade 60 steel. For this reason, the 0.2% method for finding yield stress is inappropriate for MMFX and it is suggested that ACI limitations regarding yield stress and strain not be used. Rather, the actual stress-strain relationship, determined by tensile strength tests of

MMFX, should be used when available (Dawood). Experimental testing has provided typical stress-strain relationships that have been generalized into an exponential curve fit. This provided a formula that predicts the stress in the MMFX bar at failure, as discussed in Section 2.4 below.

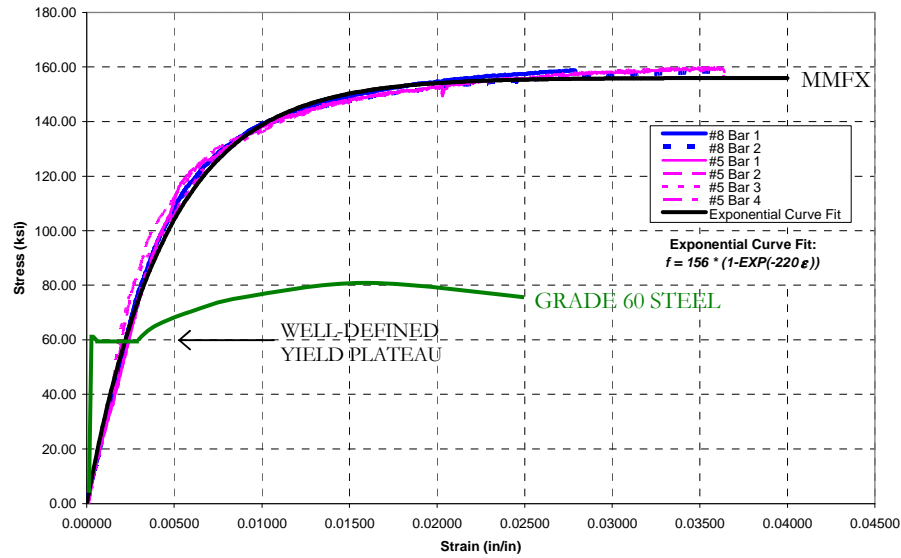


Figure 1: Stress-Strain Behavior of #5 and #8 MMFX Bars (Glass, 2006)

Also illustrating the marked difference in the modulus of elasticity (E_s) of the two materials, Figure 1 shows that Grade 60 steel has a steeper, more linear modulus than that of MMFX. As discussed further in Section 2.4, MMFX does not exhibit strength and ductility characteristics like that of conventional Grade 60 steel. Therefore, data is needed to determine how MMFX-reinforced concrete members perform when designed with ACI equations, which are intended for use with steel subjected to stresses under 80 ksi.

2.4 Coordinated Study of MMFX Bar Splices

At the University of Texas at Austin (UT), North Carolina State University (NCSU), and Kansas University (KU), coordinated projects are currently underway to study splices with MMFX steel. Parameters such as concrete cover,

concrete compressive strength, size of longitudinal bars, and amount of conventional transverse reinforcement have been shown to significantly affect the bond strength of reinforcing bars. Therefore, the coordinated study was designed to permit large variation of these parameters. By combining test data from the three research groups, the database on high-strength reinforcement will be significantly expanded (Rizkalla, 2006).

Before construction of the beams began, the specimens were first designed using material properties and equations established by the American Concrete Institute's (ACI) Building Code Requirements. However, the application of expressions involving the stress in tension steel is inappropriate, due to discrepancies between ACI's maximum allowable tensile strength (80 ksi) and the actual ultimate strength of MMFX steel (~ 160 ksi). Further complicating the matter, MMFX steel does not exhibit a well-defined yield plateau when tested in tension. Therefore, it is suggested that an exponential curve be fitted to the resulting data of tension tests, which describe the relationship between stress and strain to failure. Derived from tension tests conducted at UT by Glass, the exponential curve fit for #5 and #8 MMFX bars is:

$$f_{\text{MMFX}} = 156(1 - e^{-220\epsilon_{\text{MMFX}}})$$

where f_{MMFX} is the stress and ϵ_{MMFX} is the strain in the MMFX bar. As seen in Figure 1, these tension tests also confirmed that MMFX bars exhibit an ultimate strength nearly twice that of Grade 60 steel, as the MMFX bars consistently failed at 161 ± 1 ksi (Glass, 2006).

As ACI 408 states in the report, *Bond and Development of Straight Reinforcing Bars in Tension*, bond force in Grade 60 longitudinal bars is increased when parameters, such as concrete cover, development or splice length of longitudinal bars, spacing of longitudinal bars, and use of transverse reinforcement, are increased (ACI Committee 408, 2003). Tests conducted at NCSU confirmed that these

predictions also apply to MMFX steel. Strain gages attached to bars just outside the splice region indicated an increase in stress as confinement and splice length increased (Rizkalla 2006). While transverse reinforcement limits the progression of splitting, thus raising the bond force needed to cause failure, tests conducted at UT indicate that ACI's current code expressions underestimate effects of confinement (Glass, 2006).

3.0 Experimental Work

In order to determine if the strength of MMFX bars can be realized with splice lengths at the minimum length specified in ACI 318, several tests were conducted. Three specimens were constructed with 12 in. splices of #5 MMFX bars. The amount of confinement was varied from no transverse reinforcement to ties at 4 in. and 2.4 in. spacing.

3.1 Description of test setup and specimens as designed

The beams had a span (L) of 12 ft. and a height (h) of 12 in. The test set up is illustrated in Figure 2 below. The splices were located in the constant moment region of the beams.

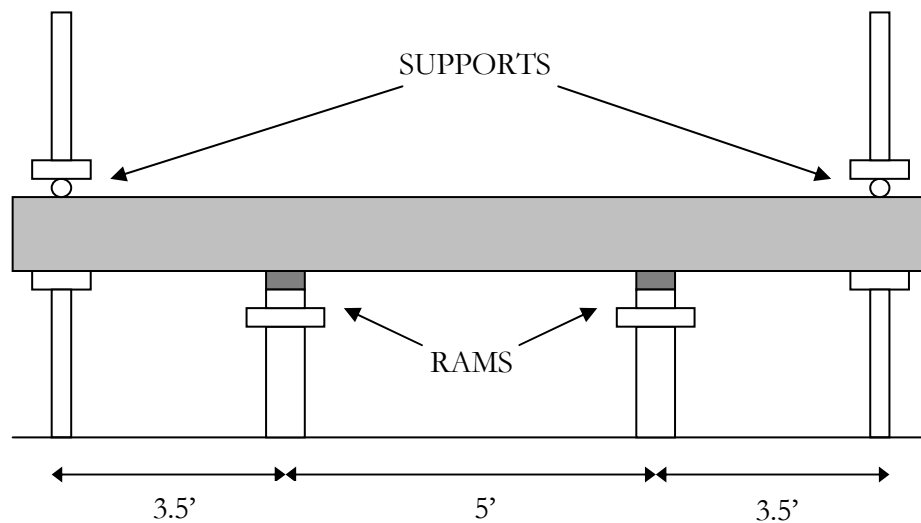


Figure 2: Test Setup

Loading the beams from underneath created compression on the bottom face of the beam and tension on the top face, which allowed the tensile cracks in the concrete to be easily viewed and marked.

#5 MMFX bars were used for tension steel and #5 Grade 60 bars were used for compression steel. The compression bars helped to ensure that the specimens

would not fail by crushing of the concrete. Failure was intended to occur within the splice region as shown in Figure 3.

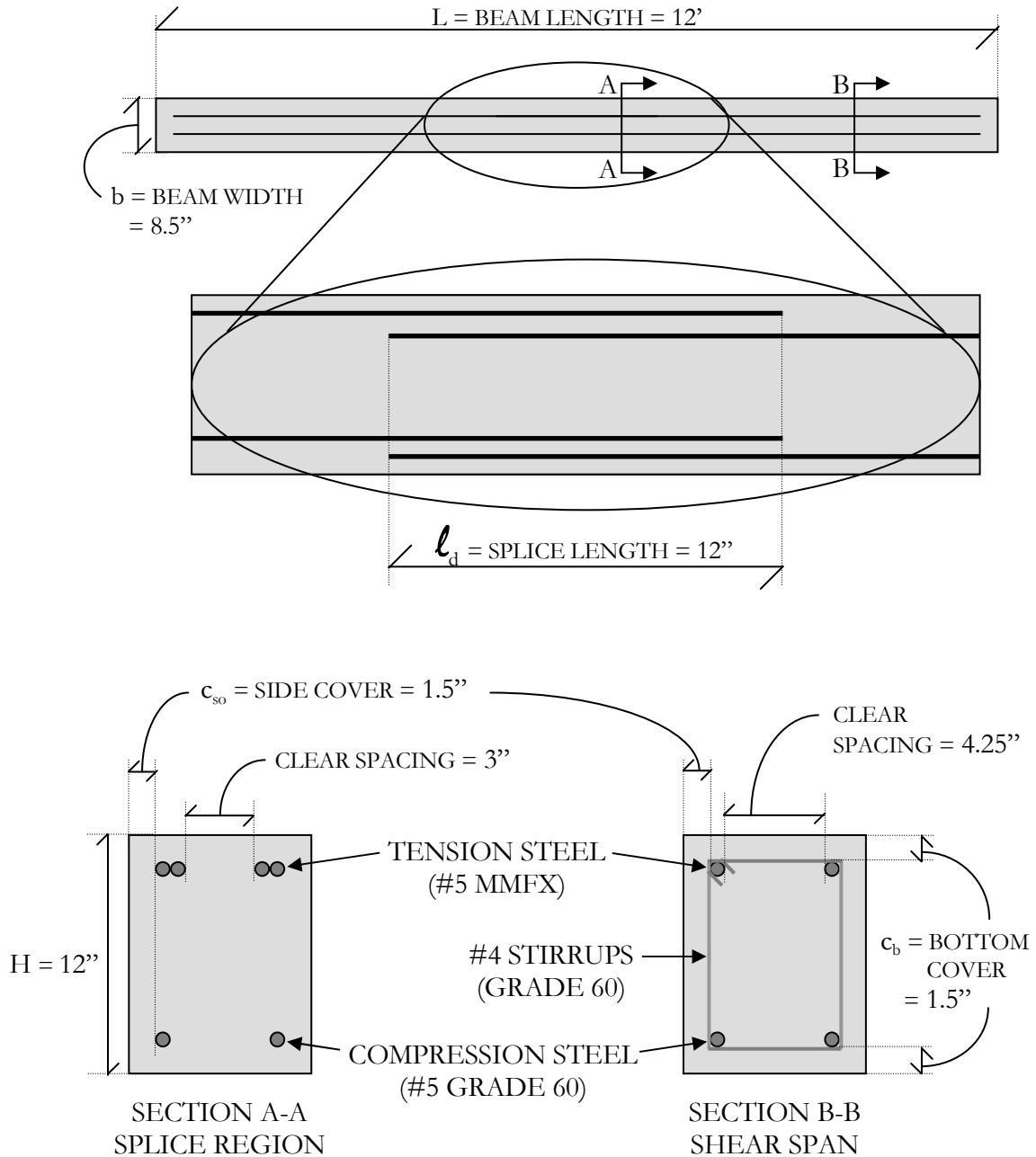


Figure 3: Plan View of Beam, Close-Up of Splice Length, and Section View for Beam C0

In an effort to avoid a shear failure, transverse reinforcement was added (Figure 4) in the shear spans between the stationary supports (reactions) and the loading rams. Conventional Grade 60 #4 stirrups were used for transverse reinforcement, spaced at 5 in., as required by the maximum stirrup spacing established by ACI ($\text{effective depth} \div 2$). The transverse reinforcement also facilitated assembly and accurate placement of the longitudinal bars.

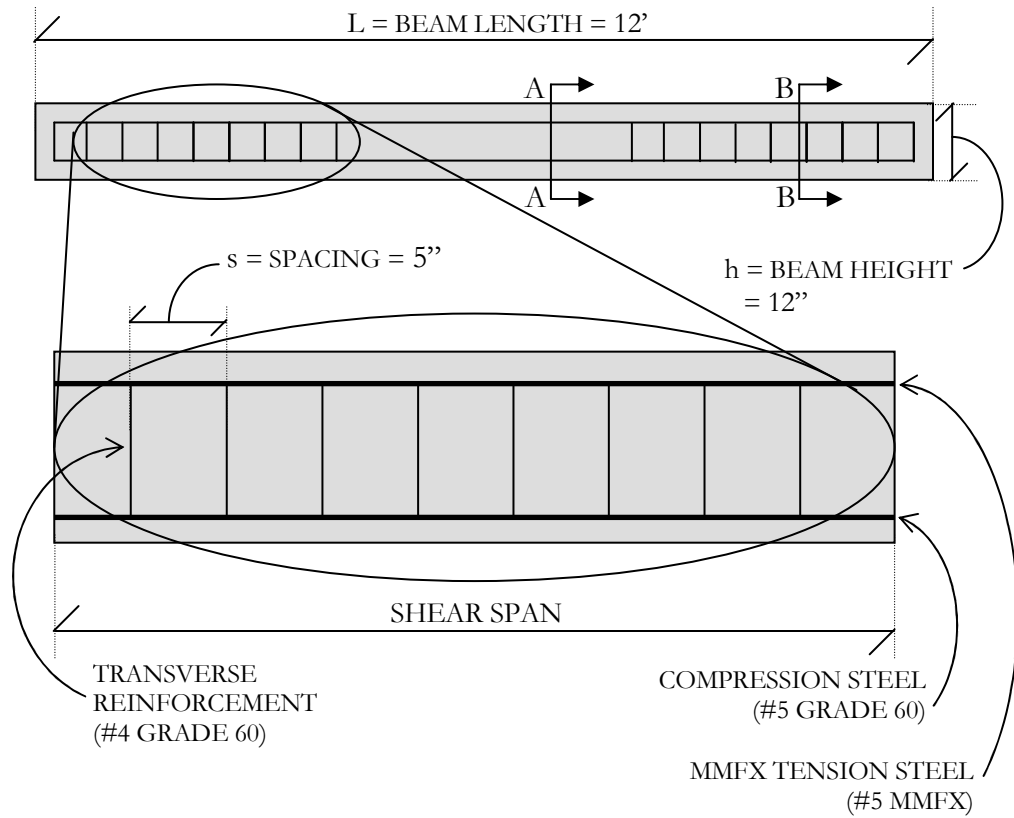


Figure 4: Elevation View of Beam and Close-Up of Shear Span

Three specimens were designed and tested. Details are shown in Table 1. The first specimen (C0) had a splice length that was unconfined and a target failure stress of approximately 50 ksi within the splice region. By limiting the maximum stress to 50 ksi, the length limit of 12 in. by ACI 318 was accommodated. Using a 12 in. splice length and ACI 408 equations, predicted failure stress was about 59

ksi. The splice length remained the same for the other two beams as well. However, the level of confinement changed as necessary to achieve the desired increase in splice strength according to ACI 408. In the second beam (C1), 3 stirrups were added in the splice length to achieve a target failure stress of about 73 ksi. Finally, the third beam (C2) was constructed with 5 stirrups in the splice length so that a target failure stress of approximately 82 ksi (neglecting limitations on the confinement term, as discussed further in Section 4.3.3) could be realized. Therefore, all three beams had the same splice length, while C0 had no transverse reinforcement, C1 had a moderate level of confinement, and C2 had a high level of reinforcement.

Beam	Splice Length (in)	Target Bar Stress* (ksi)	Transverse Reinforcement	Concrete Compressive Strength (psi)	Concrete Cover (in)		
					Side	Top	Bottom
C0	12	59	None	6027	1.5	1.5	1.5
C1	12	73	3 - #4 Stirrups	6027	1.5	1.5	1.5
C2	12	82	5 - #4 Stirrups	6027	1.5	1.5	1.5

Table 1: Details of Test Specimens

*Using ACI 408 With Unlimited Confinement Term

3.2 Construction

Once the beam dimensions had been determined, the formwork was constructed using plywood, wood studs, nails and screws, and caulk to seal the joints. The beams for this study were constructed with two beams of similar dimensions for the tests conducted by Glass, as shown in Figure 5.



Figure 5: Formwork

Next, the rebar cages were constructed, each consisting of a pair of 2 spliced #5 MMFX bars and a pair of continuous #5 Grade 60 bars, connected with #4 Grade 60 stirrups in the shear spans, as seen in Figure 6.



Figure 6: Rebar Cages

Stirrups were also placed as transverse reinforcement in the splice regions of beams C1 and C2, while C0 remained unconfined. Spaced at 4 in., C1 had three stirrups within its splice region, while C2 had five stirrups spaced at 2.4 in., as illustrated in Figure 7.

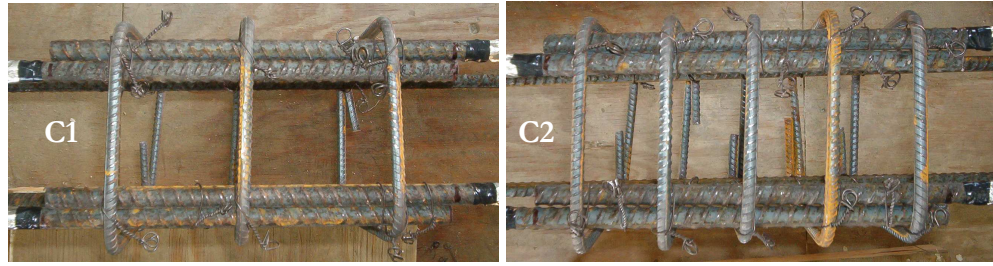


Figure 7: Close-Up of Splice Region of Rebar Cages

As shown in Figure 8, strain gauges were attached to each of the four MMFX bars, just outside of the splice, in order to monitor the steel stresses.



Figure 8: Close-Up of Strain Gauges

Once the rebar cages were completed, bar chairs were attached to the tension side of the cages and they were placed in the forms, tension side down (bottom-cast bars). Next, the concrete was placed and finished, as illustrated in Figure 9. Concrete cylinders were also made so that the compressive strength of the concrete could be monitored, so that the beams could be tested when the concrete reached design strength.



Figure 9: Placement of Concrete and Freshly Finished Beams

The setup described in Section 3.1 can be seen in Figure 10.



Figure 10: Test Setup

Once the concrete in the beams had gained enough strength, they were removed from the formwork, rotated so that the tension side faced up, and placed in the setup for testing. The strain gauges were connected to a data acquisition system and the rams were attached to a hydraulic pump. Load cells underneath the rams were also attached to the data acquisition system, and loading of the specimens was controlled by observing a load development curve on a computer monitor. An extensometer that had been placed underneath the beam was also connected to the data acquisition system so that deflection at midspan could be measured.

3.3 Testing

Load was applied to the specimens until cracking was observed on the tension side of the beams. While the load was held constant, cracks were traced, and pictures were taken. Loading continued in this fashion, with pauses after approximately 1 kip increments for crack tracing and measurement and for visual documentation. When the load approached the predicted failure stress in the spliced bars, loading was continuous until failure occurred. Pictures were taken after failure (Figure 12) and spalled concrete was used to measure actual cover dimensions. Dimensions were nearly identical to design nominal values.

4.0 Test Results and Interpretation

4.1 Results of #5 MMFX tests completed in this study

After the three beams had been tested, the measured strain in each of the spliced MMFX bars, the applied load, and displacement of the beams at midspan was compiled. Using equations of equilibrium and compatibility, this measured data was used to determine the stress in the MMFX bars at failure. The measured failure stresses were then compared to predicted failure stress calculated from ACI 408 and ACI 318 equations (found in Appendices A and B, respectively), as summarized in Table 2 below.

Beam	Confinement Term				Measured f_s (ksi)	Computed f_s (ksi)				Measured/Computed			
	ACI 408		ACI 318			ACI 408		ACI 318		ACI 408		ACI 318	
C0	2.90*	2.90	2.90*	2.50	73	59*	59	72*	62	1.25*	1.25	1.02*	1.18
C1	4.00*	4.00	4.47*	2.50	78	73*	73	111*	62	1.08*	1.08	0.71*	1.26
C2	4.73*	4.00	5.52*	2.50	84	82*	73	137*	62	1.02*	1.15	0.61*	1.35

Table 2: Results of #5 MMFX Beam Tests

*Confinement term not limited in calculation (see Section 4.3.3)

Additional data of interest includes crack widths within and near the splice regions, as well as the mode of failure that was observed during testing, and the condition of the concrete bearing area of the specimens after failure occurred. Photographs of the bearing area of C0 and C1 are shown in Figure 11 below.

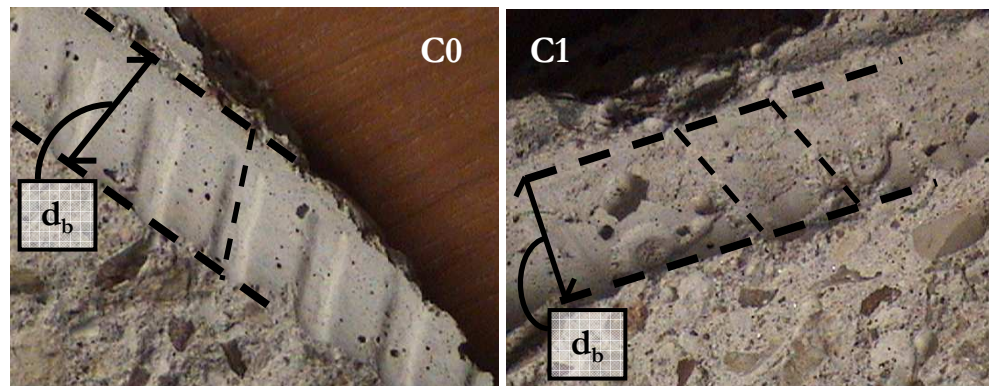


Figure 11: Close-Up of Bearing Area

Discussed further in Section 4.3.3, the concrete bearing areas of beams C0 and C1 differ physically due to different modes of failure. Whereas C0 retained indentations, left from the deformations of the rebar, the indentations in C1 have been crushed away.

The crack patterns of each beam also differ, as described in Section 4.3.3. Shown in Figure 12, C0 had longitudinal “splitting” cracks on the top (top splitting) and sides (side splitting) of the beam, as well as “v-shaped” cracking near the ends of the splices at the corners of the beams. These types of crack patterns indicate a splitting failure.

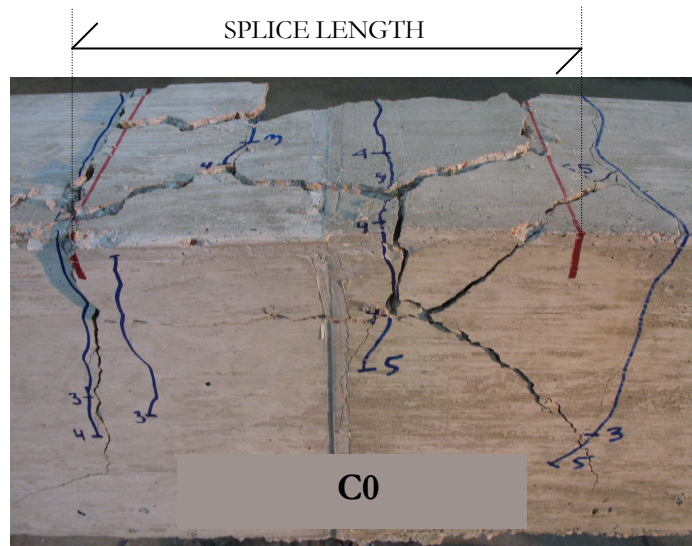


Figure 12: Close-Up of Cracking Within Splice Region of C0

Interestingly, the crack patterns of beam C1 displayed only some of the characteristic splitting cracks that were seen with C0. As seen in Figure 13 below, v-shaped cracks formed at the end of one of the splices. In addition, very little side or top splitting was observed.

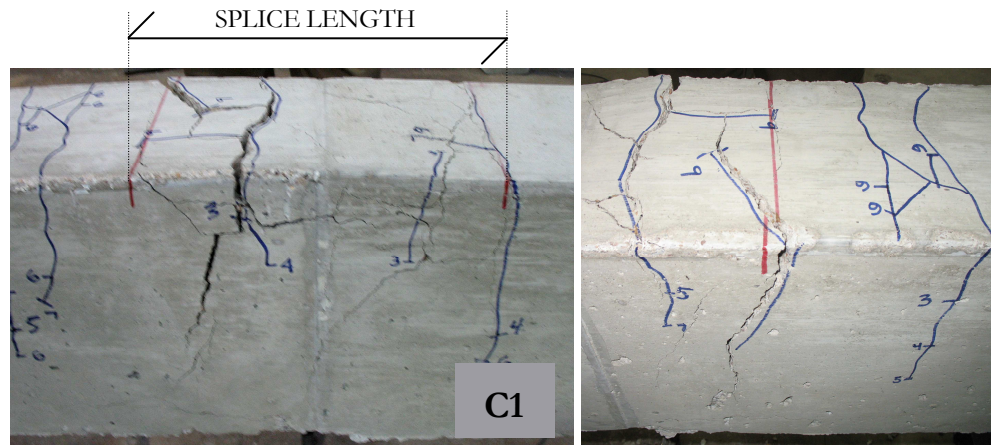


Figure 13: Close-Up of Cracking Within Splice Region of C1

Finally, C2 displayed the fewest crack patterns associated with splitting failures. Very few longitudinal splitting cracks were seen on the top of the beam (Figure 14) and there was no side splitting or v-shaped cracking observed.

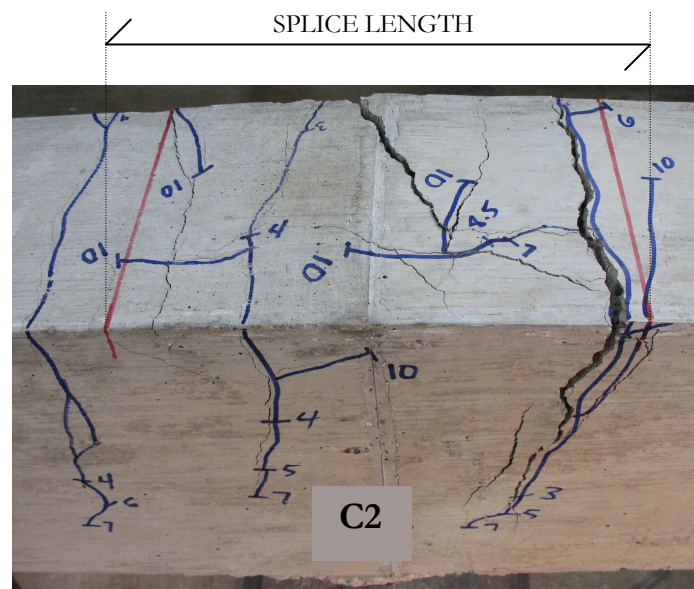


Figure 14: Close-Up of Cracking Within Splice Region of C2

4.1 Results of #5 MMFX tests (Glass, 2007)

Throughout the 2006-2007 school year, other tests involving #5 MMFX bars were completed by Greg Glass, a Master's student working under Dr. James Jirsa, at the University of Texas at Austin. While all of the #5 MMFX specimens tested by Greg Glass have unconfined splice regions, other parameters were varied, such as splice length and concrete cover; a summary of these results is provided below in Table 3.

ℓ_d (in)	c_{so} (in)	c_{si} (in)	C_b (in)	Tested f_s (ksi)	Predicted f_s (ksi)		Tested/Predicted	
					ACI 408	ACI 318	ACI 408	ACI 318
33	1.00	1.000	0.75	80	81	108	0.99	0.74
44	1.00	1.000	0.75	91	101	144	0.90	0.63
18	3.50	3.750	1.25	88	79	87	1.11	1.02
25	3.50	3.750	1.25	110	101	120	1.09	0.92
15	3.50	3.750	2.00	97	86	75	1.13	1.28
20	3.50	3.750	2.00	120	107	101	1.12	1.19

Table 3: Results of #5 MMFX Beam Tests
(Glass, 2007)

4.3 Interpretation of results

By comparing the measured failure stresses to those predicted by code equations (shown in Tables 2 and 3), several interesting trends were noticed and will be discussed separately. Members with unconfined splices are analyzed first, followed by splice length and the effects of transverse reinforcement within the splice region. Finally, the overall accuracy of predicted failure stresses will be compared for ACI 318 and ACI 408 procedures. The differences between code equations will be addressed to help explain the results.

4.3.1 Unconfined splices

For unconfined splices, both ACI 318 and ACI 408 were conservative in predicting failure stresses when splice lengths were less than 25 in. and a cover of at least 1.25 in. was provided. That is, the predicted stress at failure was always

lower than measured. With longer splices (over 25 in.), and small concrete cover, predicted values were higher than measured. This was especially true for ACI 318 values. As splice lengths increased, measured stress levels were only 61% of the predicted values. In short, the tests conducted suggest that long splice lengths of #5 MMFX bars with small concrete cover should not be used without transverse reinforcement. Since smaller diameter bars are typically used for small members or slabs in structural applications where concrete covers and transverse reinforcement are minimal, increasing splice length to achieve stresses that would take advantage of high-strength steel is not warranted.

4.3.2 Splice length

While ACI limits design stresses to 80 ksi, the test results provided in Table 3 indicate that all tested unconfined splice lengths of 15 inches or more yielded values from 80 ksi up to 120 ksi. However, not all of the predicted values within this category of moderate splice lengths were conservative, due to the varying amounts of concrete cover and lack of transverse reinforcement within the splice length. While ACI 318 resulted in values that exceeded measured values by as much as 37%, ACI 408 values exceed measured values by 10% or less. Interestingly, the equation for failure stress in ACI 408 contains an explicit strength reduction factor (ϕ) of at most 0.92; application of this factor would result in lower predicted values and ultimately would result in conservative estimates for all of the #5 specimens tested within the scope of this project. This suggests that MMFX steel may not need to be limited to 80 ksi when moderate splice lengths are used in conjunction with appropriate ϕ factors. On the other hand, strength reduction factors have been built into the ACI 318 equation to make the code more conservative. Unfortunately, this was not demonstrated in this series of tests. Instead, ACI 318 equations resulted in unconservative values despite the implicit factors of safety. In addition, ACI 318 contains an adjustment factor (ψ_s) in the calculation of failure stress that is intended to reflect more

favorable performance of bars of #6 size and smaller. This ψ_s factor allows an increase in the predicted value of stress (or a decrease in splice length). However, the results of specimens C0, C1, and C2 suggest that the use of such a factor is inappropriate when designing short splices with #5 MMFX bars, as it further increases the expected strength. Even when the ψ_s factor was left out of the failure stress computations, unconservative values of stress resulted for these three beams when the confinement term was not limited.

4.3.3 Transverse reinforcement

In an effort to investigate the change in splice strength of MMFX bars when the amount of transverse reinforcement changes, specimens C0, C1, and C2 were constructed with nearly identical parameters, varying only in the number of stirrups placed within their splice regions.

As expected, the addition of transverse reinforcement to the splice region allowed the beams to carry larger loads, and therefore higher failure stresses in the splice. Seen in Figure 15, the three beams had nearly identical deflections until maximum loading. After this point, increasing the number of stirrups in the splice region resulted in larger deflections as the confined beams began to rely on the transverse reinforcement for additional strength.

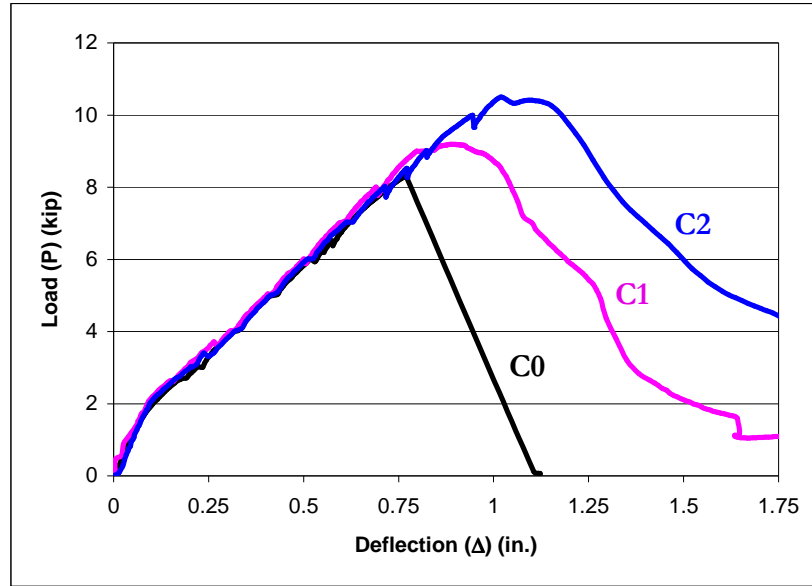


Figure 15: Load-Deflection Curves for Beams C0, C1, and C2

Due to the moderate amount of concrete cover and small bar diameter, the confinement term used in calculating the predicted failure stress began at a high value of 2.9 for C0, which is above the limit of 2.5 for ACI 318. With the introduction of and increase in transverse reinforcement, this confinement term grew larger, as is summarized in Table 4.

Beam	Confinement Term: $\frac{(c_b + K_{tr})}{d_b}$			
	ACI 408		ACI 318	
C0	2.90*†	2.90†	2.90*	2.50
C1	4.00*	4.00	4.47*	2.50
C2	4.73*	4.00	5.52*	2.50

Table 4: Confinement Terms for Predicting Failure Stresses

Note: limiting confinement terms are 2.5 (ACI 318) and 4 (ACI 408)
(values above limit suggest that pullout failure is likely)

*indicates that the confinement term is not limited

†indicates that a splitting failure is likely

In addition to contributing to the equations for predicted stress levels, this confinement term is also intended to reflect the mode of failure. The limits of 4.0

for ACI 408 and 2.5 for ACI 318 indicate that confinement terms below these limits will result in a splitting failure, whereas pullout failure will occur when the limits are exceeded. An explanation of why confinement terms differ between codes will be discussed first, followed by the accuracy to which each code predicts the mode of failure and the conservativeness of resulting failure stress predictions.

As seen in Table 4 above, the confinement terms calculated by the ACI 318 equation increase more rapidly than those calculated by ACI 408, even though the limit of the confinement term in ACI 318 is lower than that of ACI 408. This is attributed to the calculation of K_{tr} for each code (equations can be found in Appendices A and B). In ACI 408, K_{tr} is a function of the square root of the concrete compressive strength ($f_c^{1/2}$), whereas ACI 318 states that K_{tr} is a function of the strength of the transverse reinforcement (f_{yt}). Because stirrups are typically made of Grade 60 steel ($f_{yt} = 60$ ksi) and normal ranges of concrete are around 5 ksi, increases in the amount of transverse reinforcement will result in much larger values of K_{tr} when ACI 318 is used instead of ACI 408. In fact, concrete compressive strengths of at least 12.5 ksi must be used in order to achieve comparable values of K_{tr} for both codes when the number and spacing of stirrups remains constant. These proportionally larger increments of K_{tr} create larger confinement term values, and subsequently result in higher predicted failure stresses than ACI 408 predicts.

Although ACI 318 predicted pullout failures for all three of the beams, ACI 408 predicted a splitting failure for specimen C0 and a pullout failure for C2. The confinement term calculated with ACI 408 was 4.0 for C1, which is the predicted transition zone between splitting and pullout failures. Interestingly, C1 demonstrated a few signs of splitting just prior to failing in a pullout mode. Characteristics of these modes of failures can be viewed in Figures 12-14 above. Specimen C0 displayed longitudinal “splitting” cracks within the splice region and

v-shaped cracking at the ends of the splice region during testing and failed in splitting as a few chunks of concrete cover popped off the beam. In contrast, C2 had very few splitting cracks and no v-shaped cracks during testing and failed in pullout when the bearing area of the concrete against the bar deformations was unable to carry any more stress from the MMFX rebar. Demonstrating characteristics of both modes of failure, C1 displayed a couple of splitting cracks and v-shaped cracks just before failing in pullout. Although no concrete cover spalled off the specimen, a few segments were loose enough to pry off for analysis of the bearing area. As seen in Figure 11 above, the concrete bearing area of C0 remained intact with well-defined indentations where the ribs of the MMFX bars had once been, whereas the bearing area of C1 was largely destroyed as the rebar exerted excessive forces on the concrete, crushing the concrete ridges as failure occurred. Overall, ACI 408 was much more accurate in terms of predicting the mode of failure.

With the actual and limited confinement terms calculated for each specimen, the predicted failure stresses were determined for C0, C1, and C2. Although a designer would remain under the limiting value for the confinement term when calculating this stress level, it is interesting to compare tested stress values to predicted stresses that are not limited in their confinement terms. Both codes yielded conservative predictions when no transverse reinforcement was used. While ACI 408 was 25% overconservative, ACI 318 was closer to the measured failure stress for specimen C0. When stirrups were present within the splice region, values computed using ACI 408 were less than measured stresses for all beams, regardless of whether or not the confinement term was limited. Values using ACI 318 were less than measured failure stresses when the term was limited and exceeded measured failure stresses when the limit was not applied.

The data suggests that when designing beams reinforced with MMFX that have short splice lengths containing stirrups, the limit on the confinement term in ACI

318 must be applied. However, this data also implies that applying the ACI 318 upper limit when small bars and moderate cover are used results in a design that may be quite conservative. Additionally, as transverse reinforcement increased, the failure stresses predicted by ACI 318 became increasingly less accurate. In general, for beams C0, C1, and C2, ACI 408 values of stress at failure were always conservative although the ACI 408 equation was more accurate for confined splices. Likewise, ACI 318 was conservative for all three specimens when the confinement limit was applied, although the accuracy of its computed stress values decreased significantly as transverse reinforcement increased.

4.3.4 Overall Accuracy

Resulting data from the tested specimens suggest that when designing the splice strength of beams reinforced with #5 MFX bars, ACI 408 reflects the effect of cover and confinement better than ACI 318. When appropriate factors and limitations are applied, both codes generally provided safe predictions of failure stresses within the splice region, while the accuracy of each method differed as parameters, such as splice length, concrete cover, and amount of transverse reinforcement within the splice, varied. ACI 318 was most accurate and conservative when no transverse reinforcement was present within the splice region. On the other hand, the code predicted values of failure stress that were increasingly inaccurate when stirrups were introduced. In general, ACI 408 estimated failure stresses more accurately and safely, but were most conservative for splices with no transverse reinforcement. In addition, ACI 408 gave a better indication of mode of failure (splitting or pullout), especially when stirrups were introduced to the splice region. The confinement term used in ACI 408 better reflects the actual benefit of additional reinforcement. Because both methods estimated failure stresses that became less accurate as transverse reinforcement was increased, this series of tests suggest that after a certain amount of transverse

reinforcement is provided, additional reinforcement does not result in a proportional increase in splice strength.

5.0 Application to Practice

5.1 Design Recommendations

Based on the data provided by the conducted tests, it is recommended that members with spliced #5 MMFX longitudinal bars be designed by the ACI 408 method when transverse reinforcement is included within the splice region, as ACI 408 yielded safe estimates of bar strength and was more accurate than ACI 318 for the splices in this study. Designing for higher stress levels more accurately within short splice lengths results in a safe and efficient reduction in the area of steel required, thus taking advantage of high-strength steel while minimizing cost. For applications where confinement will not be included within the length of the spliced bars, it is suggested that ACI 318 may result in a more accurate design than ACI 408 would provide. Using the overconservative estimates provided by ACI 408 for unconfined splices may result in a design that requires more steel than is actually necessary to withstand target stresses. This would be wasteful and uneconomical design.

In addition, it is recommended that the confinement limit of ACI 408 (4.0) be applied in the design of confined or unconfined splices, as test results have shown that including additional transverse reinforcement does not provide a proportional increase in splice strength.

6.0 Summary and Conclusions

After testing three specimens containing spliced #5 MMFX longitudinal bars of varying levels of confinement, it was found that the values of splice strength predicted by the ACI 408 method were as safe as those estimated by ACI 318. Additionally, ACI 408 typically returned predicted values that were more accurate than ACI 318, especially when transverse reinforcement was present within the splice length. Attributed to a confinement term that better reflects the actual benefit of additional reinforcement, this suggests that higher targeted stress levels may be designed for more accurately with the ACI 408 method than when designing with ACI 318. However, testing has also shown that after a certain amount of transverse reinforcement has been added to a splice, a proportional increase in splice strength can no longer be realized.

Bibliography

- ACI Committee 318, American Concrete Institute. (2004). *Building Code Requirements for Structural Concrete (ACI 318-05) and Commentary (ACI 318R-05)*.
- ACI Committee 408, American Concrete Institute. (2003). *Bond and Development of Straight Reinforcing Bars in Tension*.
- Dawood, M.; Seliem, H.; Hassan, T.; Rizkalla, S. *Design Guidelines for Concrete Beams Reinforced with MMFX Microcomposite Reinforcing Bars*. Raleigh: North Carolina State University, Department of Civil, Construction and Environmental Engineering.
- Glass, Greg. (2006). *Bond Strength of MMFX Reinforcing Bars* (University of Texas September 2006 Progress Report). Austin: University of Texas, Center for Transportation Research, Ferguson Structural Engineering Laboratory.
- Glass, Greg. (2007). <https://webmailapp6.cc.utexas.edu/horde-2.2.9-assign/imp/view.php?thismailbox=INBOX&index=3702&> Accessed 01 March 2007.
- MMFX Technologies Corporation. (2005). <http://www.mmfx.com> Accessed 12 September 2006.
- Rizkalla, Sami. (2006). *Bond Strength of MMFX Reinforcing Bars* (Progress Report No. 2: September 2006). Raleigh: North Carolina State University, Constructed Facilities Laboratory.

Appendix A: Equations Established by ACI 408R-03

A.1 Chapter 1 – Bond Behavior

1.4 – Notation

A_b = area of bar being developed or spliced

A_{tr} = area of each stirrup or tie crossing the potential plane of splitting adjacent
to the reinforcement being developed, spliced, or anchored

c = spacing or cover dimension = $c_{min} + d_b/2$

c_b = bottom concrete cover for reinforcing bar being developed or spliced

c_{max} = maximum (c_b, c_s)

c_{min} = minimum ($c_{so}, c_b, c_{si} + d_b/2$)

c_s = minimum ($c_{so}, c_{si} + 0.25''$)

c_{si} = $1/2$ of the bar clear spacing

c_{so} = side concrete cover for reinforcing bar

d_b = diameter of bar

f_c = specified compressive strength of concrete

f_s = stress in reinforcing bar

f_y = yield strength of steel being developed or spliced

*taken as $f_{s, failure}$

f_{yt} = yield strength of transverse reinforcement

K_{tr} = transverse reinforcement index = $(0.52 t_r t_d A_{tr} / sn) f_c^{1/2}$

ℓ_d = development or splice length

n = number of bars being developed or spliced

R_r = relative rib area of the reinforcement

*taken as 0.0727 (Glass, 2006)

s = spacing of transverse reinforcement

$t_d = 0.78d_b + 0.22$

$t_r = 9.6R_r + 0.28$

α = reinforcement location factor

β = coating factor

λ = lightweight aggregate concrete factor

$$\omega = 0.1(c_{\max}/c_{\min}) + 0.9 \leq 1.25$$

A.2 Chapter 4 – Design Provisions

4.2 – ACI 408.3

$$\text{Confinement term} = (c\omega + K_{tr})/d_b \leq 4.0$$

4.3 – Recommendations by ACI Committee 408

$$\text{Equation (4-11a): } \ell_d/d_b = \{ (f_y/\phi f_c^{1/4}) - 2400\omega \} \alpha \beta \lambda / [76.3 \{ (c\omega + K_{tr})/d_b \}]$$

Appendix B: Equations Established by ACI 318-05

B.1 Chapter 2 – Notation and Definitions

2.1 – Code Notation

A_b = area of an individual bar

A_{tr} = total cross-sectional area of all transverse reinforcement within spacing s that crosses the potential plane of splitting through the reinforcement being developed

b = width of compression face of member

c_b = smaller of (a) the distance from center of a bar or wire to nearest concrete surface, and (b) one-half the center-to-center spacing of bars or wires being developed

d_b = nominal diameter of bar

f'_c = specified compressive strength of concrete

f_s = calculated tensile stress in reinforcement at service loads

f_y = specified yield strength of reinforcement

*taken as $f_{s, failure}$

f_{yt} = specified yield strength of transverse reinforcement

h = overall thickness or height of member

K_{tr} = transverse reinforcement index

ℓ = span length of beam

ℓ_d = development length in tension of deformed bar

n = number of bars

s = center-to-center spacing of transverse reinforcement

λ = modification factor related to unit weight of concrete

ψ_e = factor used to modify development length based on reinforcement coating

ψ_s = factor used to modify development length based on reinforcement size

Ψ_t = factor used to modify development length based on reinforcement location

B.2 Chapter 12 – Development and Splices of Reinforcement

12.2 – Development of Deformed Bars and Deformed Wire in Tension

12.2.1: $\ell_d \geq 12''$

$$\text{Equation (12-1): } \ell_d = \frac{(3f_y \Psi_t \Psi_s \Psi_e \lambda d_b)}{40 f_c^{1/2} \{ (c_b + K_{tr}) / d_b \}}$$

Confinement term = $(c_b + K_{tr}) / d_b \leq 2.5$

$$\text{Equation (12-2): } K_{tr} = \frac{A_{tr} f_{yt}}{1500 s_n}$$

